Synthesis and Spectroscopic Characterization of Novel Heterotermetallic Isopropoxides: X-ray Crystal Structures of $ICd\{M_2(OPr^i)_9\}$ and $[\{Cd(OPr^i)_3\}Ba\{M_2(OPr^i)_9\}]_2$ (M = Ti, Hf)†

Michael Veith,* Sanjay Mathur,* and Volker Huch

Institute of Inorganic Chemistry, University of Saarland, P.O. 151150, D-66041 Saarbrücken, Germany

Received January 31, 1996⊗

Metathesis reactions between CdI_2 and $KM_2(OPr^i)_9$ (M = Ti, Hf) in toluene produce monomeric iodo−heterobimetallic isopropoxides $ICdM_2(OPr^i)_9$ (**1,** M = Ti; **2**, M = Hf) which have been characterized by solution (^1H, ^{13}C, and ^{113}Cd) and solid state (^{13}C and ^{113}Cd) CP MAS NMR spectroscopy, microanalysis, cryoscopic molecular weight determination, and single crystal X-ray diffraction study. Both **1** and **2** in the solid state represent the first structurally characterized examples of halide heterobimetallic alkoxides based on $\{Ti_2(OPr^i)_9\}^-$ and $\{Hf_2(OPr^i)_9\}^-$ bioctahedral subunits, respectively. The overall molecular geometry of **1** and **2** can be viewed formally as an interaction of the CdI^+ fragment with $\{M_2(OPr^i)_9\}^-$ substructures *via* two terminal and two bridging (μ_2-) isopropoxy groups. Reaction of **1** and **2** with equimolar $KBa(OPr^i)_3$ in toluene afforded novel heterotermetallic isopropoxides $[\{Cd(OPr^i)_3\}Ba\{M_2(OPr^i)_9\}]_2$ (**3,** M = Ti; **4**, M = Hf). Formation of heterotermetallic frameworks involves an interesting rearrangement of the central metal atoms between the two precursor molecules, which is probably commanded by the tendency of barium to achieve higher coordination numbers. The dimeric forms of **3** and **4** as shown by cryoscopy and ^{113}Cd solution and solid state CP MAS NMR studies are confirmed by crystallography. The X-ray crystal structures of **3** and **4** reveal, as a common feature, a central $Ba(\mu_2\text{-}OPr^i)_2\text{-}Cd(\mu_2\text{-}OPr^i)_2Cd(\mu_2\text{-}OPr^i)_2Ba$ unit formed by a spirocyclic linking of two $LBa(OPr^i)_2$ (**3**, L = $Ti_2(OPr^i)_9$; **4**, L = $Hf_2(OPr^i)_9$) units to a four membered, $Cd_2(OPr^i)_2$, ring. Crystal data: for **1**, monoclinic, space group $P2_1/m$, a = 11.71(2) Å, b = 15.78(3) Å, c = 12.16(2) Å, β = 116.69(14)°, Z = 2; for **2**, triclinic, space group $P\bar{1}$, a = 9.825(2) Å, b = 11.428 Å, c = 20.619 Å, α = 95.619(12)°, β = 99.915(11)°, γ = 111.347(11)°, Z = 2; for **3**, monoclinic, space group $P2_1/c$, a = 22.68(2) Å, b = 12.603(11) Å, c = 19.00(2) Å, β = 96.83(8)°, Z = 2; for **4**, monoclinic, space group $P2_1/c$, a = 23.197(5) Å, b = 12.886(3) Å, c = 19.378(4) Å, β = 97.18(3)°, Z = 2.

Introduction

We have recently reported[1] on the synthesis and first structural characterization of a novel heterotermetallic isopropoxide $[\{Cd(OPr^i)_3\}Ba\{Zr_2(OPr^i)_9\}]_2$ supported by a face-sharing bioctahedral $Zr_2(OPr^i)_9$ substructure. The formation of $[\{Cd(OPr^i)_3\}Ba\{Zr_2(OPr^i)_9\}]_2$ as a heterotermetallic system involves an interesting exchange of central metal atoms (Cd and Ba) between the two precursors $ICd\{Zr_2(OPr^i)_9\}$ and $KBa(OPr^i)_3$. Remarkably, no major structural change or breakdown occurs in the starting molecules, and the $Zr_2(OPr^i)_9$ subunit in the obtained heterotermetallic complex binds to barium rather than cadmium as anticipated for the desired target molecule. A significant feature which becomes evident in encountering this unprecedented switching of metal atoms is the presence of a multidentate alkoxometalate unit, $Zr_2(OPr^i)_9$, in the precursor molecule, which, as a potential sequestering agent binds, with equal versatility, the different metals resulting in the formation of a thermodynamically favored heterotermetallic framework which optimally satisfies the requirements of different metal atoms. The ligating ability of the $Zr_2(OR)_9$ structural unit as observed in complexes $[ClCd\{Zr_2(OPr^i)_9\}]_2$,[2a] $(DME)KZr_2(OPr^i)_9$,[2b] and $[(Pr^iO)Ba\{Zr_2(OPr^i)_9\}]_2$[2c] is well-established in the formation of heterobimetallic systems; however, its effect in building a heterotermetallic framework has been shown for the first time.

In view of the different chemical connectivities of homoleptic alkoxides[3] of Ti and Zr, their use in obtaining heterometal alkoxide derivatives very often results in the formation of products with different metal stoichiometries as well as different structural features.[4] Also in contrast to the well-developed chemistry[5] of the $Zr_2(OPr^i)_9$ unit, the use of $MTi_2(OPr^i)_9$ (M = an alkali metal) in heterometal alkoxide chemistry has not been investigated and there are no reports available on the existence of the $Ti_2(OPr^i)_9^-$ fragment in the solid state.[6] This along with the distinct advantages[7] of titanium based mixed oxide ceramics prompted us to synthesize a heterotermetallic alkoxide containing the $M_2(OPr^i)_9$ unit based on the smaller (r (Å): Ti, 0.64; Zr, 0.80) titanium atom. While a great deal of titanium and zirconium alkoxide chemistry had been reported, the developments in hafnium alkoxide chemistry had been overshadowed largely due to an anticipated similarity of Hf compounds with Zr analogues, and reports on the synthesis and characterization of hafnium alkoxides continue to be limited. For the sake of completeness and comparison we have also synthesized and

†Dedicated to Professor Hans Georg von Schnering on his 65th birthday.

⊗ Abstract published in *Advance ACS Abstracts*, November 1, 1996.

(1) Veith, M.; Mathur, S.; Huch, V. *J. Am. Chem. Soc.* **1996,** *118*, 903.
(2) (a) Sogani, S.; Singh, A.; Bohra, R.; Mehrotra, R. C.; Nottemeyer, M. *J. Chem. Soc., Chem. Commun.* **1991,** 738. (b) Vaartstra, B. A.; Streib, W. E.; Caulton, K. G. *J. Am. Chem. Soc.* **1990,** *112*, 8593. (c) Vaartstra, B. A.; Huffman, J. C.; Streib, W. E.; Caulton, K. G. *Inorg Chem.* **1991**, *30*, 3068.
(3) Bradley, D. C.; Mehrotra, R. C.; Gaur, D. P. *Metal Alkoxides*; Academic Press: London, 1978.
(4) Hubert-Pfalzgraf, L. G. *Polyhedron* **1994,** *13* (8), 1181.
(5) Caulton, K. G.; Hubert-Pfalzgraf, L. G. *Chem. Rev.* **1990**, *90*, 969.
(6) A bonding mode similar to the $Ti_2(OPr^i)_9$ moiety has been observed in the following compounds: (a) $[Mg(\mu\text{-}Cl)_2\{Ti_2(OEt)_8Cl\}_2]$ (Malpezzi, L.; Zucchini, U.; Dall'Occo, T. *Inorg. Chim. Acta* **1991,** *180*, 245). (b) $M\{Ti_2(OEt)_9\}_2$ (M = Ba, Ca) (Turevskaya, E. P.; Kessler, V. G.; Turova, N. Y.; Pisarevsky, A. P.; Yanovsky, A. I.; Struchkov, Y. T. *J. Chem. Soc., Chem. Commun.* **1994**, 2303).
(7) Sanchez, C.; Ribot, F. *New J. Chem.* **1994**, *18*, 1007, and references cited therein.

S0020-1669(96)00116-4 CCC: $12.00

characterized by X-ray crystallography the Hf derivatives. We describe here the synthesis, characterization, and solid state molecular structures of heterotermetallic isopropoxides, $[\{Cd(OPr^i)_3\}Ba\{M_2(OPr^i)_9\}]_2$, and their precursors, $ICd\{M_2(OPr^i)_9\}$ (M = Ti, Hf).

Results and Discussion

Until recently the existence of heterotermetallic alkoxides as discrete molecular species was considered to be ambiguous. The sceptism about their identity was supported by the fact that despite extensive efforts on heterometal alkoxide chemistry by many research groups no structurally characterized example of an alkoxide cluster containing three different metals had ever been reported.[5] Also, the structurally characterized examples of halide heterometallic alkoxides which show enormous synthetic potential as precursors to multimetallic alkoxide systems are limited to a few reports.[5] As a part of our continuing research[1,8] on heteropolymetallic alkoxide systems we are interested in (i) the designing of novel alkoxometalate units and (ii) investigating their reactivity toward well-characterized halide heterobimetallic alkoxide for the purpose of studying new synthetic methods of incorporating additional metals in the molecular alkoxide assembly.

A toluene solution of $KTi_2(OPr^i)_9$ (freshly synthesized by the reaction (2:1) of $Ti(OPr^i)_4$ and $KOPr^i$ in refluxing toluene) was reacted with CdI_2 in 1:1 molar ratio by stirring (~6 h) the reaction mixture at 70 °C to obtain, after the filtration of KI and removal of solvent, the iodobimetallic isopropoxide $ICd\{Ti_2(OPr^i)_9\}$ (**1**) as a white pasty mass (95% yield). Crystallization (−30 °C) from a mixture of toluene−isopropyl alcohol gave (60%) large transparent crystals of **1**. Attempted volatilization of **1** at 110 °C and 10^{-2} Torr resulted in distillation of a colorless liquid. The elemental analysis of the distillate was consistent with $Ti(OPr^i)_4$ and was corroborated by its spectral (^1H and $^{13}C\{^1H\}$) properties identical to those of an authentic sample of $Ti(OPr^i)_4$.

In contrast to the stereochemically rigid $ICd\{Zr_2(OPr^i)_9\}$,[1] the ^1H and ^{13}C NMR spectra[8] of **1** at 20 °C are deceptively simple, indicating a rapid alkoxide site exchange in solution. The fluxional behavior of **1** is slowed down on lowering the temperature, and the best-resolved ^1H NMR spectrum obtained at −70 °C shows three resonances in the methine region which integrate 2:3:4, whereas the methyl region exhibits six doublets which integrate approximately 1:1:2:1:2:2. The solid state ^{13}C CP MAS NMR spectrum (Figure 1a) shows methine intensities in the integration ratio 2:2:1:4 which is consistent with a C_{2v} molecular symmetry in the solid state. The observed solution (δ 55.41) and solid state CP MAS ^{113}Cd NMR (δ 51.13) chemical shifts[9] are close to that observed for $ICd\{Zr_2(OPr^i)_9\}$,[1] indicating that the binding mode of the $Ti_2(OPr^i)_9$ unit to cadmium is retained in both states.

Compound **1** crystallizes in the monoclinic space group $P2_1/m$ with I, Cd, Ti(1), Ti(2), and three bridging isopropoxide oxygen atoms [O(2), O(3), O(4)] lying in the mirror plane. The molecular structure of **1** represents, to the best of our knowledge, the first structurally characterized example of a halobimetallic alkoxide based on the $Ti_2(OPr^i)_9$ structural subunit.[6] Figure 2 shows an ORTEP plot of **1** with selected atom labeling, the crystallographic data are summarised in Table 1, and relevant bond lengths and angles are given in Table 2. The central core of the molecule comprises a heterometallic $CdTi_2$ triangle in

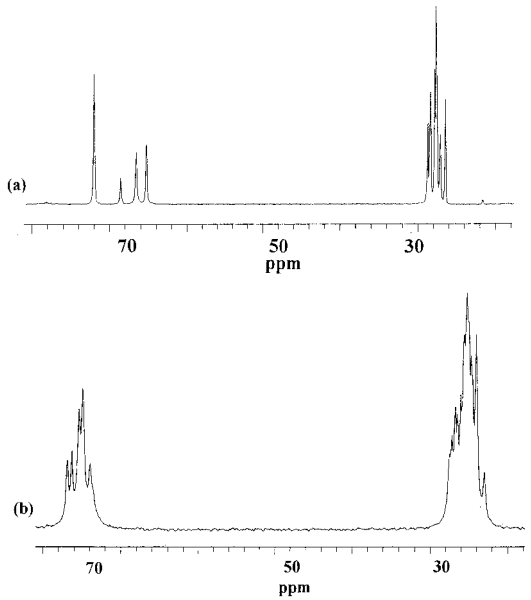

Figure 1. Solid-state ^{13}C CP MAS NMR spectra of **1** (a) and **2** (b).

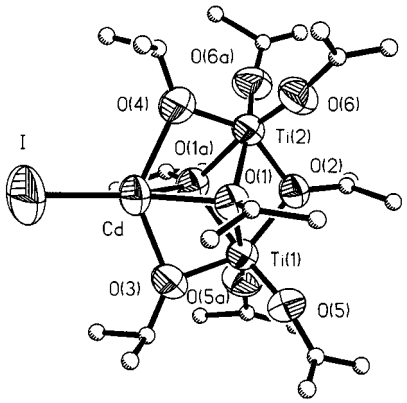

Figure 2. ORTEP drawing of $ICd\{Ti_2(OPr^i)_9\}$ (**1**), showing selected atom labeling. Atoms designated with "a" are those generated by symmetry.

which each base is capped by a μ_3-OPr^i ligand, cadmium bears a terminal iodide ligand, whereas each titanium bears two terminal isopropoxide ligands. Two Cd−Ti sides of the trimetallic core are each bridged by a μ_2-OPr^i group, while the third side, Ti−Ti, is bridged by two μ_3-OPr^i ligands. The local coordination environment around cadmium resembles a distorted trigonal bipyramid with O(3) and O(4) occupying the axial coordination sites. The Ti−O distances within the $Ti_2(OPr^i)_9$ unit show a gradation [Ti−O (terminal, μ-) < Ti−(μ_2-OTi) (doubly bridging, μ_2-) < Ti−(μ_3-OTi) (triply bridging, μ_3-)] commonly observed in the confacial bioctahedral structures of the lanthanides, actinides, and early transition metal alkoxides which provides evidence for the stability of the $Ti_2(OPr^i)_9$ subunit.[9] The average Ti−O distance (1.775 Å) displayed by the terminal isopropoxide ligands is similar to the terminal distances found in several other structurally characterized titanium alkoxides.[10] The bond distances of doubly bridging OPr^i ligands fall in two classes, depending on whether a Ti−O−Ti or Ti−O−Cd linkage is present (Table 1). Suprisingly, the Cd−(μ-OTi) distances (average 2.340 Å) in **1** are longer than the Cd−(μ_3-O) (2.281 Å) distances. The frequently observed ligating mode for the $M_2(OPr^i)_9^-$ type anions is the use of four arms (two doubly (μ_2-) and two triply (μ_3-) bridging

(8) Veith, M.; Mathur, S.; Huch, V. *J. Chem. Soc., Dalton Trans.* **1996**, 2485.
(9) Kuhlman, R.; Vaartstra, B. A.; Streib, W. E.; Huffman, J. C.; Caulton, K. G. *Inorg. Chem.* **1993**, *32*, 1272.
(10) (a) Boyle, T. J.; Bradley, D. C.; Hampden-Smith, M. J.; Patel, A.; Ziller, J. W. *Inorg. Chem.* **1995**, *34*, 5893. (b) Hampden-Smith, M. J.; Williams, D. S.; Rheingold, A. L. *Inorg. Chem.* **1990**, *29*, 4076.

Table 1. Summary of the Pertinent Crystallographic Features of Complexes **1**−**4**[a]

	1	**2**	**3**	**4**
empirical formula	$C_{27}H_{63}CdIO_9Ti_2$	$C_{27}H_{63}CdIO_9Hf_2$	$C_{72}H_{128}Ba_2Cd_2O_{24}Ti_4{\cdot}C_7H_8$	$C_{72}H_{128}Ba_2Cd_2O_{24}Hf_4{\cdot}C_7H_8$
MW	866.87	1128.05	2201.28	2723.64
cryst syst	monoclinic	triclinic	monoclinic	monoclinic
space group	$P2_1/m$	$P\bar{1}$	$P2_1/c$	$P2_1/c$
a/Å	11.71(2)	9.825(2)	22.68(2)	23.197(5)
b/Å	15.78(3)	11.428(2)	12.603(11)	12.886(3)
c/Å	12.16(2)	20.619(3)	19.00(2)	19.378(4)
β/deg	116.69(14)	99.915(11)	96.83(8)	97.18(3)
U/Å^3	2007(7)	2091.3(6)	5390(9)	5747(2)
Z	2	2	2	2
F(000)	884	1084	2276	2676
D_c/(Mg cm^{-3})	1.435	1.791	1.356	1.574
T/°C	293(2)	293(2)	293(2)	293(2)
cryst size/mm	0.6 × 0.4 × 0.3	0.5 × 0.4 × 0.2	0.5 × 0.3 × 0.2	0.68 × 0.48 × 0.06
diffractometer	Siemens Stoe AED 2	Siemens Stoe AED 2	Stoe IPDS	Stoe IPDS
scan type	$\omega-\theta$	$\omega-\theta$	$\omega-\theta$	N/A
std reflcns	3	3	50−200	50−200
θ range/deg	1.87−25.00	2.35−26.16	1.81−27.55	1.81−24.25
reflcns collcd	3675	7684	8873	35982
independ reflcns	3675	7684	8873	9129
obsd reflcns	3014	6481	6409	6620
GOF on F^2	1.249	1.26	1.280	1.022
final R indicies [R_1; $I > 2\sigma(I)$]	0.0514	0.0531	0.0880	0.0598
R indicies (R_1; all data)	0.0616	0.0605	0.1113	0.0801
hydrogen atoms	geom	geom	geom	geom

[a] Details in common: Programs used, SHELXS-86[26a] and SHELXS-93;[26b] refinement method, full-matrix least-squares on F^2; radiation, graphite monochromator.

Table 2. Selected Interatomic Distances (Å) and Angles (deg) for $ICdTi_2(OPr^i)_9$ (**1**)[a,b]

Cd−I	2.644(6)	Cd−O(1)	2.281(5)
Cd−O(1′)	2.281(5)	Cd−O(3)	2.337(7)
Cd−O(4)	2.343(6)	Ti(1)−O(5)	1.774(4)
Ti(1)−O(5′)	1.774(4)	Ti(1)−O(2)	2.041(5)
Ti(1)−O(1′)	2.167(5)	Ti(1)−O(1)	2.167(5)
Ti(2)−O(6)	1.775(4)	Ti(2)−O(4)	1.925(7)
Ti(2)−O(2)	2.047(7)	Ti(2)−O(1)	2.157(4)
Ti(2)−O(1′)	2.107(4)		
O(1′)−Cd−O(1)	65.5(2)	O(1′)−Cd−O(3)	70.2(2)
O(1)−Cd−O(3)	70.2(2)	O(1′)−Cd−O(4)	69.9(2)
O(3)−Cd−O(4)	132.2(2)	O(1)−Cd−O(4)	69.9(2)
O(1′)−Cd−I	138.65(13)	O(1)−Cd−I	155.79(9)
O(3)−Cd−I	115.2(2)	O(4)−Cd−I	112.1(2)
O(1′)−Cd−I′	155.79(9)	O(1)−Cd−I′	138.65(13)
O(3)−Cd−I′	115.2(2)	O(4)−Cd−I′	112.1(2)
O(5′)−Ti(1)−O(5)	98.9(3)	O(5′)−Ti(1)−O(3)	99.9(2)
O(5)−Ti(1)−O(3)	99.9(2)	O(5′)−Ti(1)−O(2)	100.5(2)
O(5)−Ti(1)−O(2)	100.5(2)	O(3)−Ti(1)−O(2)	148.3(2)
O(5′)−Ti(1)−O(1′)	95.8(2)	O(5)−Ti(1)−O(1′)	165.0(2)
O(2)−Ti(1)−O(1′)	73.6(2)	O(3)−Ti(1)−O(1)	80.5(2)
O(5′)−Ti(1)−O(1)	165.0(2)	O(5)−Ti(1)−O(1)	95.8(2)
O(3)−Ti(1)−O(1)	80.5(2)	O(2)−Ti(1)−O(1)	73.6(2)
O(1′)−Ti(1)−O(1)	69.4(2)	O(6′)−Ti(2)−O(6)	98.4(3)
O(6′)−Ti(2)−O(4)	100.0(2)	O(6)−Ti(2)−O(4)	100.0(2)
O(6′)−Ti(2)−O(2)	100.3(2)	O(6)−Ti(2)−O(2)	100.3(2)
O(4)−Ti(2)−O(2)	148.7(2)	O(6′)−Ti(2)−O(1′)	95.8(2)
O(6)−Ti(2)−O(1′)	165.4(2)	O(4)−Ti(2)−O(1′)	80.8(2)
O(2)−Ti(2)−O(1′)	73.7(2)	O(6′)−Ti(2)−O(1)	165.4(2)
O(6)−Ti(2)−O(1)	95.8(2)	O(4)−Ti(2)−O(1)	80.8(2)
O(2)−Ti(2)−O(1)	73.7(2)	O(1′)−Ti(2)−O(1)	69.8(2)
Ti(2)−O(1)−Ti(1)	91.6(2)	Ti(2)−O(1)−Cd	91.7(2)
Ti(1)−O(1)−Cd	91.6(2)	Ti(1)−O(2)−Ti(2)	98.6(3)
Ti(1)−O(3)−Cd	96.2(2)	Ti(2)−O(4)−Cd	96.0(3)

[a] The primed atoms in this table are the ones represented by "a" in Figure 2. [b] The primed atoms are generated from the unprimed ones by the symmetry operation $x, -y + {}^1/_2, z$.

alkoxide oxygens) to form a basket for accommodating the heterometal atom, which in the case of **1** is not appropriate (for Cd^{2+}) in size (bigger!), presumably due to the much shorter Ti−OPr^i (terminal) distances, and ultimately result in two long (μ_2-OPr^i bonds) and two short (μ_3-OPr^i bonds) Cd−OTi contacts. The structurally characterized heterometal alkoxides based on the $\{M_2(OR)_9\}^-$ unit generally show a trend in which the length of the bonding interaction of the alkoxide oxygen of the $M_2(OR)_9^-$ unit to the central metal atom increases with each successive bridging which is due to the loss of electron density at the alkoxide oxygen.[11] In view of the above one expects the values to follow the order observed for the alkoxides bridging titanium atoms in **3**: μ_3-OR > μ_2-OR > OR. The structurally related actinide derivatives $KU_2(O^tBu)_9$ [12] and $NaTh_2(O^tBu)_9$ [13] reported by Cotton and Clark, respectively, show a similar observation with alkali metal−oxygen distances for doubly bridging (μ_2-) alkoxides being longer than the triply bridging ones. However, in the two actinide structures, the alkali metals have no terminal ligands, whereas, in compound **1**, cadmium bears an electronegative substituent (iodide) that may tend to pull the cadmium away from the Ti−Ti vector, which along with the shorter Ti−O (terminal) distances will make the doubly bridging interactions longer than the triply bridging ones.

$KHf_2(OPr^i)_9$ was obtained in a manner analogous to $KZr_2(OPr^i)_9$ by the equimolar reaction of $Hf_2(OPr^i)_8(Pr^iOH)_2$ and KOPr^i in benzene as a white solid soluble in common organic solvents which sublimes at 150 °C/10^{-2} Torr and has been characterized by elemental analysis, cryoscopy, and multinuclear NMR spectral studies (see Experimental Section). A reaction (1:1) of anhydrous CdI_2 with freshly sublimed $KHf_2(OPr^i)_9$ in toluene by continuous stirring at 70 °C for ∼4 h offered, after a workup of the reaction, $ICdHf_2(OPr^i)_9$ (**2**) in quantitative yield. The low-temperature (−30 °C) crystallization from a mixture of toluene−hexane led to the isolation of colorless crystals of **2** in 50% yield. In contrast to **1**, compound **2** exhibits remarkable thermal stability and could be sublimed at 155 °C/10^{-2} Torr in high yield. The spectral properties of **2** are very close to the Zr analogue,[1] and the ^{1}H NMR spectrum of **2** in C_6D_6 at ambient temperature correlates to the presence of four

(11) Vaartstra, B. A.; Samuels, J. A.; Barash, E. H.; Martin, J. D.; Streib, W. E.; Gasser, C.; Caulton, K. G. *J. Organomet. Chem.* **1993**, *449*, 191.
(12) Cotton, F. A.; Marler, D. O.; Schwotzer, W. *Inorg. Chem.* **1984,** *23*, 4211.
(13) Clark, D. L.; Watkin, J. G. *Inorg. Chem.* **1993,** *32*, 1766.

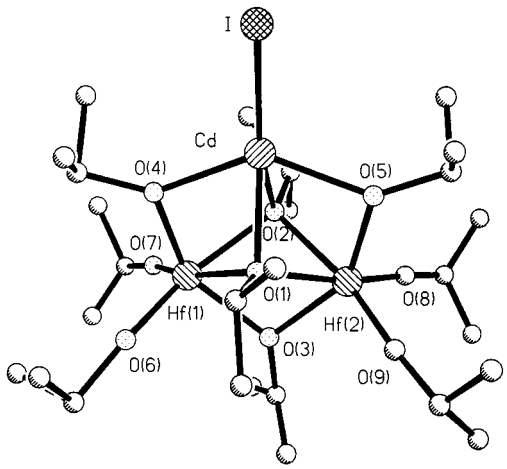

Figure 3. Ball and stick drawing of $ICd\{Hf_2(OPr^i)_9\}$ (**2**) with the atom numbering scheme.

types of alkoxide environments in the molecule. However, in contrast to the sharp doublet observed for the four terminal OPr^i groups of $ICdZr_2(OPr^i)_9$,[1] the signal corresponding to the methyl protons of the terminal OPr^i groups in **2** appears as two doublets which probably arise from a partially hindered rotation of isopropyl groups around M−O bonds. The above spectral observation of the nonfluxional behavior of **2** can be correlated to a better fit of Cd^{2+} in the basket formed by four alkoxide oxygens of the $Hf_2(OPr^i)_9$ unit (*vide supra*). The room temperature ^{13}C NMR spectrum exhibits four well-defined resonances in the methine region with integration ratio 4:1:2:2, which suggests that **2** has a *pseudo-*C_{2v} symmetry in solution. The cryoscopic molecular weight determination ($\eta = 1.1$) showed the presence of **2** as a monomeric species in solution. The chemical ionization mass spectrum (M^+) of crystalline **2** exhibits a molecular ion corresponding to the monomer, and a mass consistent with the loss of an isopropoxy group from **2** is observed at *m*/*e* (%) = 1069 (100%), where "*m*" corresponds to high abundance isotopes for all of the elements. Indeed, compound **2** is monomeric in the solid state, and a ball and stick drawing of the molecule with atom numbering scheme is shown in Figure 3. The crystallographic features are presented in Table 1, whereas the selected bond distances and bond angles are given in Table 3. The solid state structure of **2** is essentially similar to that of Ti and Zr analogues and may formally be viewed as an anionic face-sharing bioctahedral $\{(Pr^iO)_3Hf(\mu\text{-}OPr^i)_3Hf(OPr^i)_3\}^-$ unit coordinating to a cationic CdI^+ unit through four oxygen atoms of the isopropoxy groups, two of which also bridge the two Hf atoms. Bond lengths from Hf to OPr^i follow the order Hf−O (terminal) (1.915(7)−1.923(8) Å) < Hf−(μ_2-OCd) (2.030(7)−2.043(6) Å) < Hf−(μ_2-OHf) (2.168(6)−2.173(6) Å) < Hf−(μ_3-OPr^i) (2.255(5)−2.277(5) Å). The average Hf−O distances (1.919 Å) displayed by terminal isopropoxide ligands are similar to the terminal distances found in the structures of $[Hf(OPr^i)_4(Pr^iOH)]_2$ [14] and $[Hf(OPr^i)_4Py]_2$.[14] The three doubly bridged OPr^i groups are planar at the oxygens (angles sum to 359.6−359.9°). Each hafnium is six-coordinate but there are significant distortions from the regular octahedral geometry (Figure 3); the *trans* O−Hf−O angles range from 144.2 to 164.6°, whereas *cis* angles are found in the range from 67.5 to 102.6°. The Cd−I distance (2.6284(12) Å) is significantly shorter than the sum of their van der Waals radii and explains the covalent and volatile nature of **2**. Unlike **1**, there is no mirror plane present in the solid state structure of **2** and all isopropoxy groups are crystallographically different. This loss of symmetry in the $M_2(OR)_9$ substructure of **2** (Figure 3) is observable in the solid state ^{13}C CP MAS NMR spectrum (Figure 1b). The $M_2(OR)_9$ structural unit is of common occurrence in alkoxide chemistry as observed in the X-ray crystal structures of $ICdSn_2(OPr^i)_9$,[8] $ICdZr_2(OPr^i)_9$,[1] $NaCe_2(O^tBu)_9$,[15] $KU_2(O^tBu)_9$,[12] and $NaTh_2(O^tBu)_9$;[13] however, no such reports are available for hafnium, and **2** represents the first structurally characterized halide heterometal alkoxide derivative based on a $Hf_2(OPr^i)_9^-$ unit.

Table 3. Selected Interatomic Distances (Å) and Angles (deg) for $ICdHf_2(OPr^i)_9$ (**2**)

Cd−I	2.6284(12)	Hf(1)−O(6)	1.915(7)
Hf(1)−O(4)	2.043(6)	Hf(1)−O(2)	2.261(5)
Hf(2)−O(8)	1.916(8)	Hf(2)−O(5)	2.030(7)
Hf(2)−O(1)	2.255(5)	Hf(1)−O(7)	1.922(7)
Hf(1)−O(3)	2.173(6)	Hf(1)−O(1)	2.277(5)
Hf(2)−O(9)	1.923(8)	Hf(2)−O(3)	2.168(6)
Hf(2)−O(2)	2.261(5)	Cd−O(4)	2.306(6)
Cd−O(1)	2.315(6)	Cd−O(2)	2.329(6)
Cd−O(5)	2.361(7)		
O(6)−Hf(1)−O(7)	99.8(3)	O(7)−Hf(1)−O(4)	102.6(3)
O(7)−Hf(1)−O(3)	101.8(3)	O(6)−Hf(1)−O(2)	162.6(3)
O(4)−Hf(1)−O(2)	78.8(2)	O(6)−Hf(1)−O(1)	95.3(3)
O(4)−Hf(1)−O(1)	77.0(2)	O(2)−Hf(1)−O(1)	67.5(2)
O(8)−Hf(2)−O(5)	100.7(3)	O(8)−Hf(2)−O(3)	100.6(3)
O(5)−Hf(2)−O(3)	145.6(2)	O(9)−Hf(2)−O(1)	96.9(3)
O(3)−Hf(2)−O(1)	73.0(2)	O(9)−Hf(2)−O(2)	164.6(3)
O(3)−Hf(2)−O(2)	72.6(2)	O(6)−Hf(1)−O(4)	100.2(3)
O(6)−Hf(1)−O(3)	100.9(3)	O(4)−Hf(1)−O(3)	144.2(2)
O(7)−Hf(1)−O(2)	97.3(3)	O(3)−Hf(1)−O(2)	72.5(2)
O(7)−Hf(1)−O(1)	164.6(3)	O(3)−Hf(1)−O(1)	72.5(2)
O(8)−Hf(2)−O(9)	99.0(4)	O(9)−Hf(2)−O(5)	101.4(3)
O(9)−Hf(2)−O(3)	101.5(3)	O(8)−Hf(2)−O(1)	163.9(3)
O(5)−Hf(2)−O(1)	79.1(2)	O(8)−Hf(2)−O(2)	96.2(3)
O(5)−Hf(2)−O(2)	78.6(2)	O(1)−Hf(2)−O(2)	67.9(2)
O(4)−Cd−O(1)	71.4(2)	O(1)−Cd−O(2)	65.8(2)
O(1)−Cd−O(5)	71.6(2)	O(4)−Cd−O(2)	72.4(2)
O(4)−Cd−O(5)	135.8(2)	O(2)−Cd−O(5)	71.0(2)
O(4)−Cd−I	113.5(2)	O(2)−Cd−I	146.62(14)
O(1)−Cd−I	147.53(14)	O(5)−Cd−I	110.7(2)
Hf(2)−O(1)−Hf(1)	93.6(2)	Hf(2)−O(1)−Cd	92.2(2)
Hf(2)−O(2)−Hf(1)	93.9(2)	Hf(2)−O(2)−Cd	91.7(2)
Hf(2)−O(3)−Hf(1)	99.1(2)	Hf(2)−O(5)−Cd	97.0(2)
Hf(1)−O(1)−Cd	91.5(2)	Hf(1)−O(2)−Cd	91.6(2)
Hf(1)−O(4)−Cd	98.1(2)		

The quest for soluble alkoxides of alkaline earth metals, especially barium, has gained additional impetus due to its presence in many of the high-T_c superconductors, such as $YBa_2Cu_3O_{7-x}$,[16] $HgBa_2CuO_4$,[17] and $Ba_{0.6}K_{0.4}BiO_3$,[18] and also due to their potential application in the synthesis of perovskite oxide phases such as $BaTiO_3$ which is used in high-dielectric constant capicator materials. However, in most of the cases attempts made to synthesize well-defined homo- or heterometal alkoxides of barium have resulted in the formation of oxo complexes or high-nuclearity aggregrates.[19] More studies have shown that these metals exhibit a pronounced tendency to form molecular aggregates stabilized by either oxo, hydroxo, water, other suitable Lewis bases, or solvent molecules, e.g., $[H_4Ba_6(O)(OCH_2CH_2OMe)_{14}]$,[20] $[HBa_5(O)(OPh)_9(thf)_8]$,[21] $[Ba_6(OPh)_{12}(TMEDA)_4]$,[22] $[Ba_4Ti_4O_4(OPr^i)_{16}(Pr^iOH)_x]$,[23]

(14) Veith, M.; Mathur, S. Results to be published.

(15) Evans, W. J.; Deming, T. J.; Olofson, J. M.; Ziller, J. W. *Inorg. Chem.* **1989,** *28*, 4027.
(16) Rupich, M. W.; Lagos, B.; Hachey, J. P. *Appl. Phys. Lett.* **1989,** *55*, 2447.
(17) Putlin, S. N.; Antipov, E. V.; Chmaissem, O.; Marezio, M. *Nature* **1993,** *363*, 56.
(18) Mattheiss, L. F.; Gyorgy, E. M.; Johnson, D. W. *Phys. Rev. B* **1988,** *37*, 3745.
(19) Mehrotra, R. C.; Singh, A.; Sogani, S. *Chem. Soc. Rev.* **1994**, 215.
(20) Caulton, K. G.; Chisholm, M. H.; Drake, S. R.; Huffman, J. C. *J. Chem. Soc., Chem. Commun.* **1990,** 1498.

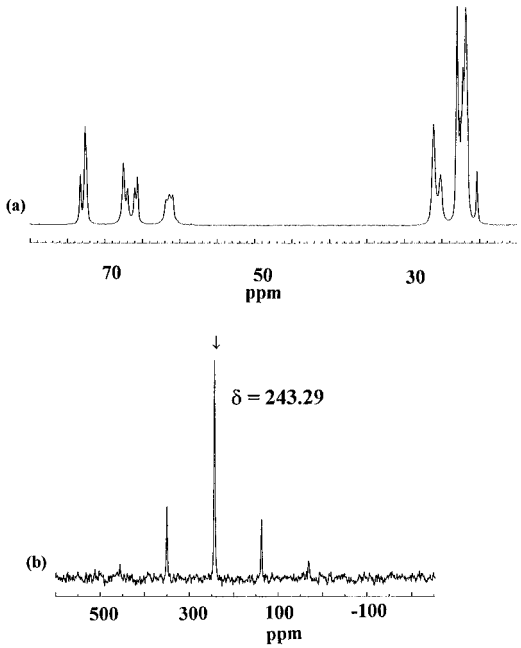

Figure 4. Solid state CP MAS ^{13}C (a) and ^{113}Cd NMR (b) spectra of **3**. The arrow indicates the isotropic shift for ^{113}Cd, all other lines being the spinning side bands.

$[Ba_4(O)(OC_6H_2(CH_2NMe_2)_3\text{-}2,4,6)_6](toluene)_3$.[24] In order to minimize the problems of the formation of oxo complexes and nuclear aggregates, we have attempted to achieve a better tailoring scheme for incorporation of barium in heterometallic alkoxide systems by employing a novel alkoxometalate unit $Ba(OPr^i)_3^-$ toward well-characterized halide heterobimetallic alkoxides. This strategy elucidates a reproducible synthesis of stoichiometrically precise heterotermetallic frameworks and has been successfully employed to other alkaline earth metals, e.g., Sr, Ca, and Mg, which is the subject of a separate publication.[14]

Compound **1** reacts with freshly synthesized $KBa(OPr^i)_3$ [1] in toluene at room temperature (~12 h) to afford, after the workup, a white solid in 97% yield (eq 1); the product was dissolved in

$$\underset{\mathbf{1}\ M = Ti;\ \mathbf{2}\ M = Hf}{ICd\{M_2(OPr^i)_9\}} + KBa(OPr^i)_3 \rightarrow \underset{\mathbf{3}\ M = Ti;\ \mathbf{4}\ M = Hf}{^1/_2[\{Cd(OPr^i)_3\}Ba\{M_2(OPr^i)_9\}]_2} + KI \quad (1)$$

a mixture of toluene−pentane and cooled (−8 °C) to obtain (40% yield) colorless plates of $[\{Cd(OPr^i)_3\}Ba\{Ti_2(OPr^i)_9\}]_2$ (**3**). The heterotermetallic nature of **3** was unambiguously established by a single crystal X-ray analysis which shows it to be a centrosymmetric dimer in the solid state. An ORTEP representation of **3** is shown in Figure 5; the crystallographic data and some pertinent bond lengths and angles are presented in Tables 1 and 4, respectively. In contrast to the simple spectroscopic features exhibited by precursor **1**, the room temperature ^1H and ^{13}C NMR spectra of **3** are informative of the structural pattern existing in solution. The ^1H NMR spectrum of **3** in C_6D_6 exhibits methyl intensities in an integration ratio 2:1:4:2:2:1 which support the contention that the molecule retains its heterotermetallic nature in the solution; the methine protons are observed as three overlapping septets with integrals of 5:3:4. The ^{13}C NMR spectrum displays eight signals each for methine and methyl carbons, respectively. The ^{13}C CP MAS NMR (Figure 4) spectrum shows nine signals for the methine carbons in intensity ratio 2:6:4:2:2:2:2:2:2 whose total intensities are consistent with the expected pattern for a static molecule of **3**. The retention of the dimeric structure of **3** in solution is indicated by the cryoscopic molecular weight measurements in benzene ($\eta = 1.8$) and is further supported

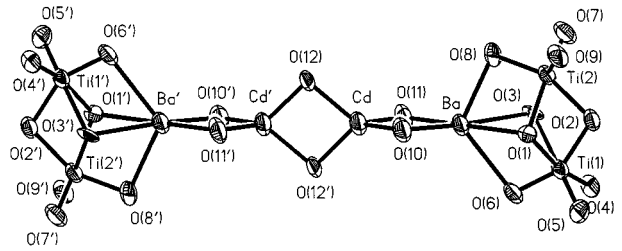

Figure 5. ORTEP representation of the central metal−oxygen framework of **3**. All oxygen atoms bear isopropyl groups which have been omitted for clarity. Atoms labeled with a prime are related by symmetry.

Table 4. Selected Bond Lenghts (Å) and Angles (deg) for $[\{Cd(OPr^i)_3\}Ba\{Ti_2(OPr^i)_9\}]_2$ (**3**)[a]

Ba−O(10)	2.337(5)	Ba−O(3)	2.422(5)
Ba−O(8)	2.556(6)	Ba−O(11)	2.617(6)
Ba−O(6)	2.702(6)	Ba−O(1)	2.802(6)
Cd−O(12′)	1.959(6)	Cd−O(11)	2.033(6)
Cd−O(12)	2.132(6)	Cd−O(10)	2.280(6)
Ti(2)−O(7)	1.799(7)	Ti(2)−O(8)	1.806(6)
Ti(2)−O(9)	1.868(7)	Ti(2)−O(2)	2.013(6)
Ti(2)−O(1)	2.108(6)	Ti(2)−O(3)	2.160(6)
Ti(1)−O(4)	1.752(7)	Ti(1)−O(6)	1.732(6)
Ti(1)−O(2)	1.925(6)	Ti(1)−O(5)	1.979(7)
Ti(1)−O(1)	2.061(6)	Ti(1)−O(3)	2.303(6)
O(12)−Cd(1′)	1.959(5)		
O(10)−Ba−O(3)	161.3(2)	O(10)−Ba−O(8)	101.3(2)
O(3)−Ba−O(8)	65.7(2)	O(10)−Ba−O(11)	83.4(2)
O(3)−Ba−O(11)	113.3(2)	O(8)−Ba−O(11)	115.5(2)
O(10)−Ba−O(6)	118.5(2)	O(3)−Ba−O(6)	62.9(2)
O(8)−Ba−O(6)	116.4(2)	O(11)−Ba−O(6)	116.5(2)
O(10)−Ba−O(1)	102.9(2)	O(3)−Ba−O(1)	60.8(2)
O(8)−Ba−O(1)	65.2(2)	O(11)−Ba−O(1)	173.5(2)
O(6)−Ba−O(1)	59.2(2)	O(12′)−Cd−O(11)	119.7(3)
O(12′)−Cd−O(12)	85.7(3)	O(11)−Cd−O(12)	113.9(3)
O(12′)−Cd−O(10)	114.2(3)	O(11)−Cd−O(10)	99.8(2)
O(12)−Cd−O(10)	125.2(2)	O(7)−Ti(2)−O(8)	88.0(3)
O(7)−Ti(2)−O(9)	106.7(4)	O(8)−Ti(2)−O(9)	100.7(3)
O(7)−Ti(2)−O(2)	107.0(3)	O(8)−Ti(2)−O(2)	154.2(3)
O(9)−Ti(2)−O(2)	95.0(3)	O(7)−Ti(2)−O(1)	164.6(3)
O(8)−Ti(2)−O(1)	95.1(2)	O(9)−Ti(2)−O(1)	87.6(3)
O(2)−Ti(2)−O(1)	65.1(2)	O(7)−Ti(2)−O(3)	88.2(3)
O(8)−Ti(2)−O(3)	83.9(3)	O(9)−Ti(2)−O(3)	164.4(3)
O(2)−Ti(2)−O(3)	76.0(2)	O(1)−Ti(2)−O(3)	77.2(2)
O(4)−Ti(1)−O(6)	93.5(3)	O(4)−Ti(1)−O(2)	102.1(3)
O(6)−Ti(1)−O(2)	151.4(3)	O(4)−Ti(1)−O(5)	102.3(3)
O(6)−Ti(1)−O(5)	101.6(3)	O(2)−Ti(1)−O(5)	98.4(3)
O(4)−Ti(1)−O(1)	163.1(3)	O(6)−Ti(1)−O(1)	91.3(3)
O(2)−Ti(1)−O(1)	67.5(2)	O(5)−Ti(1)−O(1)	92.6(3)
O(4)−Ti(1)−O(3)	89.7(3)	O(6)−Ti(1)−O(3)	82.0(3)
O(2)−Ti(1)−O(3)	74.3(2)	O(5)−Ti(1)−O(3)	167.2(3)
O(1)−Ti(1)−O(3)	74.9(2)	Ti(1)−O(1)−Ti(2)	94.1(2)
Ti(1)−O(1)−Ba	88.9(2)	Ti(2)−O(1)−Ba	83.0(2)
Ti(1)−O(2)−Ti(2)	101.5(3)	Ti(2)−O(3)−Ti(1)	86.2(2)
Ti(2)−O(3)−Ba	91.8(2)	Ti(1)−O(3)−Ba	93.7(2)
Ti(1)−O(6)−Ba	99.7(3)	Ti(2)−O(8)−Ba	96.7(2)
Cd−O(10)−Ba	89.3(2)	Cd−O(11)−Ba	87.5(2)
Cd(1′)−O(12)−Cd	94.3(3)		

[a] The primed atoms are generated from the unprimed ones by the symmetry operations $-x + 2, -y, -z + 2$ and $-x, -y + 1, -z$.

(21) Caulton, K. G.; Chisholm, M. H.; Drake, S. R.; Huffman, J. C. *J. Chem. Soc., Chem. Commun.* **1990,** 1349.
(22) Caulton, K. G.; Chisholm, M. H.; Drake, S. R.; Folting, K.; Huffman, J. C. Streib, W. E. *Inorg. Chem.* **1993,** *32,* 1970.
(23) Yanovsky, A. I.; Yanovskaya, M. I.; Limar, V. K.; Kessler, V. G.; Turova, N. Y.; Struchkov, Y. T. *J. Chem. Soc., Chem. Commun.* **1991,** 1605.
(24) Tesh, K. F.; Hanusa, T. P. *J. Chem. Soc., Chem. Commun.* **1991,** 879.

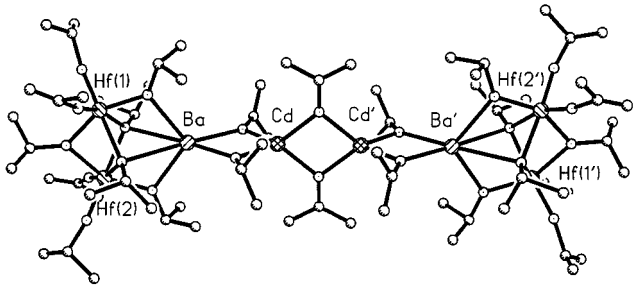

Figure 6. Ball and stick drawing of the centrosymmetric dimeric structure of **4**. Hydrogen atoms have been omitted for clarity, and atoms labeled with a prime are related by symmetry.

by the observed ^{113}Cd NMR chemical shifts in solid (δ 243.29, Figure 4b) and solution (δ 241.74) states, which as observed in the case of Zr derivative[1] correspond to a four-coordinated cadmium.

In a similar procedure, $[\{Cd(OPr^i)_3\}Ba\{Hf_2(OPr^i)_9\}]_2$ (**4**) was obtained quantitatively by the equimolar reaction (eq 1) of **2** with $KBa(OPr^i)_3$ in toluene. Ambient temperature ^{1}H and ^{13}C NMR spectra of **4** indicate that the molecule is stereochemically rigid. The ^{1}H NMR spectrum shows six doublets which integrate 2:2:1:2:3:2 and are consistent with the pattern expected for **4**; the methine protons are observed as overlapping septets. This observation is corroborated by the ^{13}C NMR spectrum which displays six methine resonances with a 4:1:2:2:1:2 ratio; the methyl region shows eight signals. Interestingly, the solution ^{113}Cd NMR chemical shift of **4** (δ 238.03) is similar to that observed for $[\{Cd(OPr^i)_3\}Ba\{Zr_2(OPr^i)_9\}]_2$ (δ 237.12).[1] The central spiro unit $Ba(\mu\text{-}OPr^i)_2Cd(\mu\text{-}OPr^i)_2Cd(\mu\text{-}OPr^i)_2Ba$ is the same in both Zr and Hf derivatives, and owing to the almost similar ionic radii of Zr^{4+} (0.80 Å) and Hf^{4+} (0.86 Å) no marked difference is exerted on the local coordination environment of cadmium, which is not directly bound by the $\{M_2(OPr^i)_9\}$ framework. It is noteworthy that ^{113}Cd NMR chemical shifts observed for the precursor molecules $ICd\{Zr_2(OPr^i)_9\}$ (δ 67.21) and $ICd\{Hf_2(OPr^i)_9\}$ (δ 52.99), where the cadmium coordination environment is directly influenced by the Zr and Hf centers are significantly different. In view of the small difference in the electronegativities of Zr^{4+} and Hf^{4+}, the difference ($\sim$14 ppm) in the chemical shifts of iodo-derivatives indicates the extreme sensitivity of the cadmium chemical shifts to the immediate coordination environment, which has proved to be a valuable tool in studying the structural behavior of these derivatives in solution and the solid state. Molecular weight measurements show **4** to be dimeric in freezing benzene (+5 °C). The single crystals of **4** were grown from a cold (−12 °C) toluene solution and subjected to X-ray diffraction analysis. A ball and stick drawing of the molecular structure of **4** is shown in Figure 6, and the important bond lengths and angles are given in Table 5.

Compounds **3** and **4** exist as centrosymmetric dimers in the solid state (Figures 5 and 6). Both are isostructural and permit a concurrent discussion of the salient crystallographic features and their comparison with the related Zr complex, $[\{Cd(OPr^i)_3\}Ba\{Zr_2(OPr^i)_9\}]_2$ (**5**) (Table 6). Compounds **3**−**5** are the first structurally characterized examples of molecular alkoxide assemblies containing three different metals. The formation of the heterotermetallic framework in all three derivatives observes an unprecedented exchange of central metal atoms between the constituting fragments which can formally be represented as $Cd\{M_2(OPr^i)_9\}^+$ (M = Ti, Zr, Hf) and $Ba(OPr^i)_3^-$. In view of the larger radii of ions of heavier alkaline earth metals [Ca^{2+}, 1.00 Å; Sr^{2+}, 1.18 Å; Ba^{2+}, 1.35 Å][25] they remain coordinatively unsaturated with the ligands of relatively smaller size (e.g., OPr^i, OEt, OMe) and their compounds, $[M(OR)_2]_n$, often spontaneously oligomerize resulting in polymeric products. Such an unsaturation is likely to be present in "$Ba(OPr^i)_3^-$" species, which in the absence of any coordinating solvent in the reaction system (the presence of which would be a source for achieving higher coordination numbers) coupled with the greater oxophilicity (in comparison to Cd^{2+}) of Ba^{2+} induces a rearrangement of metals to form a stable heterotermetallic system in which Ba displays a higher (6) coordination number. Analogous to the Zr derivative, the structures of $[\{Cd(OPr^i)_3\}Ba\{Ti_2(OPr^i)_9\}]_2$ and $[\{Cd(OPr^i)_3\}Ba\{Hf_2(OPr^i)_9\}]_2$ exhibit a one dimensional array of Ba···Cd···Cd···Ba atoms lying on a 2-fold axis in the metal−oxygen framework of the central $Ba(\mu_2\text{-}OPr^i)_2Cd_2(\mu_2\text{-}OPr^i)_2Ba(\mu_2\text{-}OPr^i)_2$ unit. The overall molecular structures of both **3** and **4** can be viewed as a spirocyclic linking of two $Ba(OPr^i)_2L$ (**3**, L = $\{Ti_2(OPr^i)_9\}^-$; **4**, L = $\{Hf_2(OPr^i)_9\}^-$) units to a $Cd_2(OPr^i)_2$ four-membered ring. Alternatively, it can be described as a combination of two triangular $BaM_2(\mu_2\text{-}OPr^i)_2(\mu_3\text{-}OPr^i)_3(\mu\text{-}OPr^i)_4^+$ units which are joined together by a $[(Pr^iO)_2Cd(\mu_2\text{-}OPr^i)_2Cd(OPr^i)_2]^{2-}$ unit. The triangular repre-

Table 5. Selected Bond Lengths (Å) and Angles (deg) for $[\{Cd(OPr^i)_3\}Ba\{Hf_2(OPr^i)_9\}]_2$ (**4**)[a]

Ba−O(1)	2.825(6)	Ba−O(2)	2.837(7)
Ba−O(4)	2.733(8)	Ba−O(5)	2.774(8)
Ba−O(11)	2.549(9)	Ba−O(10)	2.556(8)
Cd−O(12′)	2.177(9)	Cd−O(11)	2.154(9)
Cd−O(12)	2.160(8)	Cd−O(10)	2.168(8)
Hf(1)−O(7)	1.896(8)	Hf(1)−O(6)	1.907(9)
Hf(1)−O(4)	2.018(8)	Hf(1)−O(3)	2.173(8)
Hf(1)−O(2)	2.237(6)	Hf(1)−O(1)	2.246(7)
Hf(2)−O(9)	1.903(8)	Hf(2)−O(8)	1.919(8)
Hf(2)−O(5)	2.019(8)	Hf(2)−O(3)	2.168(8)
Hf(2)−O(1)	2.225(7)	Hf(2)−O(2)	2.232(6)
O(12)−Cd(1′)	2.177(9)		
O(11)−Ba−O(10)	72.9(3)	O(11)−Ba−O(4)	122.8(3)
O(10)−Ba−O(4)	105.8(3)	O(11)−Ba−O(5)	112.9(3)
O(10)−Ba−O(5)	121.2(3)	O(4)−Ba−O(5)	114.9(2)
O(11)−Ba−O(1)	123.5(2)	O(10)−Ba−O(1)	162.7(2)
O(4)−Ba−O(1)	61.8(2)	O(5)−Ba−O(1)	60.6(2)
O(11)−Ba−O(2)	173.8(3)	O(10)−Ba−O(2)	111.2(2)
O(4)−Ba−O(2)	61.2(2)	O(5)−Ba−O(2)	61.2(2)
O(1)−Ba−O(2)	53.0(2)	O(11)−Cd−O(12)	125.1(4)
O(11)−Cd−O(12′)	122.4(3)	O(12)−Cd−O(10)	121.8(3)
O(10)−Cd−O(12′)	123.5(4)	O(11)−Cd−O(10)	89.2(3)
O(12)−Cd−O(12′)	79.6(4)	Hf(2)−O(1)−Hf(1)	94.1(2)
O(7)−Hf(1)−O(6)	99.5(4)	O(7)−Hf(1)−O(4)	100.7(4)
O(6)−Hf(1)−O(4)	97.8(4)	O(7)−Hf(1)−O(3)	99.4(3)
O(6)−Hf(1)−O(3)	99.8(4)	O(4)−Hf(1)−O(3)	150.7(3)
O(7)−Hf(1)−O(2)	164.7(3)	O(6)−Hf(1)−O(2)	94.4(4)
O(4)−Hf(1)−O(2)	83.5(3)	O(3)−Hf(1)−O(2)	71.9(3)
O(7)−Hf(1)−O(1)	97.0(4)	O(6)−Hf(1)−O(1)	162.7(4)
O(4)−Hf(1)−O(1)	84.0(3)	O(3)−Hf(1)−O(1)	72.5(3)
O(2)−Hf(1)−O(1)	68.7(2)	O(9)−Hf(2)−O(8)	97.1(4)
O(9)−Hf(2)−O(5)	102.3(4)	O(8)−Hf(2)−O(5)	98.8(4)
O(9)−Hf(2)−O(3)	96.5(4)	O(8)−Hf(2)−O(3)	100.4(4)
O(5)−Hf(2)−O(3)	151.1(3)	O(9)−Hf(2)−O(1)	96.1(3)
O(8)−Hf(2)−O(1)	165.8(3)	O(5)−Hf(2)−O(1)	83.3(3)
O(3)−Hf(2)−O(1)	73.0(3)	O(9)−Hf(2)−O(2)	163.2(3)
O(8)−Hf(2)−O(2)	97.0(3)	O(5)−Hf(2)−O(2)	84.3(3)
O(3)−Hf(2)−O(2)	72.1(3)	O(1)−Hf(2)−O(2)	69.1(2)
Hf(2)−O(1)−Ba	95.6(2)	Hf(1)−O(1)−Ba	94.6(2)
Hf(2)−O(2)−Hf(1)	94.2(2)	Hf(2)−O(2)−Ba	95.1(2)
Hf(1)−O(2)−Ba	94.5(2)	Hf(2)−O(3)−Hf(1)	97.8(3)
Hf(1)−O(4)−Ba	103.1(3)	Hf(2)−O(5)−Ba	102.4(3)
Cd−O(10)−Ba	98.7(3)	Cd−O(11)−Ba	99.2(3)
Cd−O(12)−Cd′	100.4(4)		

[a] The primed atoms are generated from the unprimed ones by the symmetry operations $-x, -y+1, -z+2$ and $-x, -y+2, -z+2$.

(25) Hanusa, T. P. *Chem. Rev.* **1993**, *93*, 1023.

Table 6. Comparison of Important Crystallographic Features (Bond Lengths (Å), Angles (deg)) for a Set of $[\{Cd(OPr^i)_3\}Ba\{M_2(OPr^i)_9\}]_2$ (M = Ti, Zr, and, Hf) Type Heterotrimetallic Systems

	$[\{Cd(OPr^i)_3\}Ba\{M_2(OPr^i)_9\}]_2$ bond lengths and angles for given M (ionic radius/Å)		
	Ti^{4+} (0.64)	Zr^{4+} (0.80)	Hf^{4+} (0.86)
Ba−(μ_2-OPr^i(M))	2.629(6)	2.699(11)	2.754(8)
Ba−(μ_3-OPr^i(M))	2.612(6)	2.719(9)	2.831(7)
Ba−(μ_2-OPr^i(Cd))	2.477(5)	2.521(11)	2.552(9)
Cd−O(12)	2.132(6)	2.179(11)	2.160(8)
Cd−O(12′)	1.959(6)	1.979(11)	2.177(9)
M−OPr^i	1.849(7)	2.044(12)	1.906(8)
M−(μ-OPr^i)	1.969(6)	2.146(11)	2.018(8)
M−(μ_3-OPr^i)	2.124(6)	2.320(10)	2:235(7)
bite angle at Ba formed by			
(i) two μ-OPr^i	116.4(2)	120.5(3)	114.9(2)
(ii) two μ_3-OPr^i	60.8(2)	60.9(3)	53.0(2)
Ba−O(10)−Cd	89.3(2)	87.9(4)	98.7(3)
Ba−O(11)−Cd	87.5(2)	86.6(4)	99.2(3)
O(10)−Ba−O(11)	83.4(2)	84.5(4)	72.9(3)
O(10)−Cd−O(11)	99.8(2)	101.1(4)	89.2(3)
O(12)−Cd−O(12′)	85.7(3)	86.4(5)	79.6(4)
Cd′−O(12)−Cd	94.3(3)	93.6(5)	100.4(4)
M−O−C	154.5(13)−171(2)	169.3(10)−178(2)	166(2)−170(2)
M−(μ-OPr^i)−Ba	97.9(5)	99.4(4)	102.75

sentation as emphasized in the view selected for compound **1** (Figure 2) provides a conceptual link to the carrying over of structural features from precursor to compound **2**. As observed in the case of **5**, each barium, titanium, and hafnium atom in **3** and **4** is six-coordinate. Despite the fact that the six ligands are all isopropoxides, the distortions in the octahedral geometry of these metal atoms are mainly due to the constraints imposed by the $M_2(OR)_9$ framework. A molecule of toluene, which serves as a space filler, is found in the crystal lattice of both **3** and **4**, but it shows no interaction with the complex (closest contact > 3.6 Å). The cadmium atom is quasi-tetrahedral in all three derivatives. In comparison to **4** and **5**, the observed Cd−O(12′) distance in **3** is considerably shorter, indicating a lesser extent of asymmetric bridging (Table 6); however, in compound **4** the Cd−O(12) (2.160(8) Å) and Cd−O(12′) (2.177(9) Å) distances are comparable. The observed Cd−O(12′) distances (Table 6) in **3**−**5** are significantly shorter than an average Cd−O dative bond and thus consistent with their dimeric forms.

The short terminal M−O bonds (M = Ti, Zr, and Hf) and obtuse M−O−C angles as observed in the $M_2(OPr^i)_9$ unit of all the three (**3**−**5**) derivatives (Table 6) are a feature of frequent occurrence among the alkoxides of early transition metals and indicate the oxygen π-donation to M^{4+}. However, we have recently observed that linearization of the M−O−C angle in electropositive elements is not necessarily an evidence for the degree of π-bonding and may result from a high degree of ionic character.[8] Although the M−O−C angles for the terminal OPr^i groups in **3** are more deviated from linearity in comparison to the Hf derivative ($\angle$Ti−O−C = 154.5(13)−177(2)°; $\angle$Hf−O−C = 166(2)−170(2)°), the shorter Ti−O bonds in **3** are mainly due to the smaller size and enchanced electrophilicity of Ti centers.

Interestingly, in contrast to Zr^{4+}, the larger Hf^{4+} shows smaller M−O bonds associated with relatively smaller angles (Table 6). As observed in the precursor molecules, the M−O distances in the $M_2(OR)_9$ unit of **3**−**5** increase in the order M−O(terminal) < M−(μ-OBa) < M−(μ_2-OM) < M−(μ_3-OM), the trend among three derivatives being $Ti^{4+} < Hf^{4+} < Zr^{4+}$. Owing to the inherent size effect, all M−O bond distances in the $M_2(OPr^i)_9$ unit are uniformly shorter for **2** in comparison to Zr complex and longer in **4**. In contrast to the trend observed for the M−OR distances in **3**−**5**, the Ba−(μ-O)−M angles have a reverse order for **4** and **5** (average Ba−(μ-O)−M, 98.2° in **3**, 99.4° in **4**, and 102.8° in **5**). This observation is a constraint of the triangular $\{BaM_2(OPr^i)_9\}^+$ framework, and its compensation results in the narrowing of the *trans* O−Ba−O angles (**3**, 116.4°; **4**, 114.9°; **5**, 120.5°), which as a consequence and as observed for the iodo derivatives **1** and **2** make the Ba−(μ_2-OM) bonds longer than those of Ba−(μ_3-OM). Associated with the short terminal Ti−O distances in **3** are very long distances of μ_2- and μ_3-isopropoxide oxygens to barium which are nearly the same for Ti (average Ba−(μ_2-OTi) = 2.663 Å and Ba−O(1) = 2.858(11) Å) in comparison to the larger Zr (average Ba−(μ_2-OZr) = 2.699 Å and Ba−O(1) = 2.947(10) Å) and Hf (average Ba−(μ_2-OHf) = 2.753(8) Å and Ba−O(1) = 2.825(6) Å) atoms, which corroborates the reported[3] thermal instability of the $MTi_2(OPr^i)_9$ (M = Na, K) compounds in contrast to the volatile $MM'_2(OPr^i)_9$ (M′ = Zr, Hf) derivatives.

Experimental Section

X-ray Diffraction: General Information. In an atmosphere of dry and deoxygenated nitrogen a suitable crystal was affixed to the end of a glass fiber using silicone grease and transferred to a quartz capillary of appropriate dimensions. The sealed capillary was then mounted on the goniometer head of a four circle diffractometer (Siemens AED for **1** and **2**) or an image plate system (STOE for **3** and **4**). The lattice constants were refined using 20 reflections with 2θ ranging between 20 and 25°. In all of the structure determinations, Mo Kα radiation (λ = 0.7107 Å) and a graphite monochromator together with an $\omega-\theta$ scan (only in the case of **1** and **2**) was used. After correction of Lorentz and polarization effects, the data were averaged to yield a set of unique intensities and σ's. The structures were solved by direct methods.[26] Hydrogen atoms were geometrically fixed to the carbon atoms, and the overall refinement method used was full-matrix least squares on F^2. Crystal data and details on data collection and refinement for **1**−**4** are collected in Table 1, whereas results of the structure determination are presented in Tables 2−5.

All manipulations were performed under a dry and deoxygenated dinitrogen atmosphere. All hydrocarbon solvents were distilled under an inert atmosphere from sodium benzophenone ketyl. Isopropyl alcohol was dried by distillation from magnesium turnings and aluminum triisopropoxide. $Ti(OPr^i)_4$ (Aldrich) was purified by distil-

(26) (a) Sheldrick, G. M. *Programme for Crystal Structure Determination, SHELXS-86*; University of Göttingen: Göttingen, Germany, 1986. (b) Sheldrick, G. M. Programme for Crystal Structure Determination. *SHELXL-93*; University of Göttingen: Göttingen, Germany, 1993.

lation. $[Hf(OPr^i)_4(Pr^iOH)]_2$[3] was synthesized according to the literature method. $KTi_2(OPr^i)_9$ and $KHf_2(OPr^i)_9$ were prepared by the reaction of potassium isopropoxide with $Ti(OPr^i)_4$ and $[Hf(OPr^i)_4(Pr^iOH)]_2$, respectively, in appropriate molar ratios in toluene and benzene, respectively. Cadmium iodide was dried by heating *in vacuo* and analyzed for cadmium and iodine contents before use. NMR spectra were recorded on a Bruker AC-200 NMR spectrometer by using protio impurities of the deuterated solvents as reference for ^{1}H NMR and ^{13}C resonance of the solvents as reference for ^{13}C NMR. ^{113}Cd NMR chemical shifts in solution and solid state are referenced externally to a 0.1 M solution of $Cd(NO_3)_2$ in D_2O and solid $Cd(NO_3)_2\cdot 4H_2O$, respectively. ^{13}C and ^{113}Cd CP MAS NMR spectra were recorded on a Bruker MSL 200S spectrometer. Elemental analyses (C and H) were performed by using a LECO Elemental Analyzer CHN 900. Standard analytical procedures[27] were employed to estimate metal and iodine contents in the complexes. Molecular weights were determined cryoscopically by the freezing point depression of benzene.

$ICdTi_2(OPr^i)_9$ (1). A toluene (30 mL) solution of $KTi_2(OPr^i)_9$ (obtained by the reaction of $KOPr^i$ (1.73 g, 17.61 mmol) and $Ti(OPr^i)_4$ (10.02 g, 35.23 mmol) in toluene at 70 °C) was added slowly to a suspension of anhydrous CdI_2 (6.40 g, 17.47 mmol) in toluene (20 mL) followed by the continuous stirring of the reaction mixture for ~12 h at 50 °C. The preciptated KI was filtered off. The volatiles were removed *in vacuo* to yield a viscous mass which analyzed to $ICdTi_2(OPr^i)_9$ (**1**). The compound is highly soluble in toluene (20 mL) in the presence of a little amount of isopropyl alcohol (2 mL), and the resulting solution when left to stand overnight at −30 °C produced large crystals (8.70 g, 60%) of **1**. Anal. Calcd for $C_{27}H_{63}CdIO_9Ti_2$: C, 37.38; H, 7.27; I, 14.64; Cd, 12.97; Ti, 11.05. Found: C, 37.21; H, 7.09; I, 14.60; Cd, 12.81; Ti, 11.07. ^{1}H NMR (200.13 MHz, 20 °C, C_6D_6): δ 4.51 (septet, 9H, $^3J_{H-H}$ = 6 Hz), 1.25 (d, 54H, $^3J_{H-H}$ = 6 Hz). $^{13}C\{^1H\}$ NMR (50.3 MHz, 20 °C, C_6D_6): δ 75.82 (*C*H), 26.23 (*C*H3). ^{1}H NMR (200.13 MHz, C_7D_8, −70 °C): methine peaks at δ 4.96 (br septet, $^3J_{H-H}$ = 6 Hz, 2H), 4.78 (septet, $^3J_{H-H}$ = 6 Hz, 3H), 4.64 (septet, $^3J_{H-H}$ = 6Hz, 4H); six methyl peaks as doublets (approximate intensity 1:1:2:1:2:2) at δ 1.62, 1.54, 1.40, 1.36, 1.28, and 1.24. $^{13}C\{^1H\}$ NMR (50.3 MHz, C_7D_8, −70 °C): δ 79.39, 76.55, 74.16, 71.61 (*C*H); 26.62, 20.63 (CH_3). ^{13}C CP MAS NMR: δ 79.57, 75.49, 73.12, 71.58 (*C*H); 28.36, 27.98, 27.28, 27.08, 26.45, 25.65 (CH_3). ^{113}Cd NMR: δ 55.41. ^{113}Cd CP MAS NMR: δ 51.13.

(I) Synthesis of $KHf_2(OPr^i)_9$. To a solution of $KOPr^i$, freshly prepared by dissolving potassium (0.41 g, 10.48 mmol) in a mixture of isopropyl alcohol (10 mL) and benzene (15 mL) was added a benzene (40 mL) solution of $[Hf(OPr^i)_4(Pr^iOH)]_2$ (9.94 g, 10.46 mmol). The mixture was refluxed with stirring for ~6 h. All solvent was removed *in vacuo* to leave a white solid which could be sublimed (150−155 °C/10^{-2} Torr) in 70% yield. Anal. Calcd for $C_{27}H_{63}O_9Hf_2K$ (%): C, 34.91; H, 6.79; Hf, 38.47. Found (%): C, 35.14; H, 6.88; Hf, 37.98. The cryoscopic molecular weight values measured at two different concentrations were 1037 and 998. The calculated value for $KHf_2(OPr^i)_9$ is 928. ^{1}H NMR (200.13 MHz, 20 °C, C_6D_6): δ 1.53 (d, $^3J_{H-H}$ = 6 Hz, 6H), 1.46 (d, $^3J_{H-H}$ = 6 Hz, 12H), 1.43 (d, $^3J_{H-H}$ = 6 Hz, 12H), 1.38 (d, $^3J_{H-H}$ = 6 Hz, 12H), 1.18 (d, $^3J_{H-H}$ = 6 Hz, 12H) (CH_3); 4.66 (sept, J = 6 Hz, 6H), 4.50 (sept, J = 6 Hz, 3H) (*C*H). $^{13}C\{^1H\}$ NMR (50.3 MHz, 20 °C, C_6D_6): δ 69.90, 68.39, 67.52, 67.26, 66.92 (*C*H); δ 27.96, 27.48, 27.33, 26.60, 26.40 (CH_3).

(II) $ICdHf_2(OPr^i)_9$ (2). A benzene solution of freshly sublimed $KHf_2(OPr^i)_9$ (5.72 g, 6.16 mmol) in benzene (25 mL) was added to a prestirred suspension of CdI_2 (2.26 g, 6.17 mmol) in benzene (20 mL). After stirring the reaction mixture for ~6 h at 70 °C, the resulting suspension was filtered and volatiles were removed under reduced pressure to yield a white solid (6.67 g, 97%). Dissolving the solid in a minimum amount of a mixture of toluene−pentane followed by cooling to −30 °C gave (3.40 g, 51%) large transparent crystals of $ICdHf_2(OPr^i)_9$ (**2**). The product is extremely hydrocarbon soluble, and crystallization leaves much of the product in solution. Another 20% of crystalline **2** could be recovered by recooling a concentrated mother liquor. Anal. Calcd for $C_{27}H_{63}CdIO_9Hf_2$: C, 28.72; H, 5.58; I, 11.25; Cd, 9.96; Hf, 31.64. Found: C, 28.59; H, 5.61; I, 11.16; Cd, 9.72; Hf, 30.58. Mol. Wt. Calcd for **2:** 1128. Found: 1195, 1203. ^{1}H NMR (200.13 MHz, 20 °C, C_6D_6): δ, 1.24 (d, $^3J_{H-H}$ = 6 Hz, 12H), 1.25 (d, $^3J_{H-H}$ = 6 Hz, 12H), 1.31 (d, $^3J_{H-H}$ = 6 Hz, 6H), 1.45(d, $^3J_{H-H}$ = 6 Hz, 12H), 1.52 (d, $^3J_{H-H}$ = 6 Hz, 12H) (CH_3); 4.42 (sept, $^3J_{H-H}$ = 6 Hz, 4H), 4.60 (sept, $^3J_{H-H}$ = 6 Hz, 3H), 4.77 (sept, $^3J_{H-H}$ = 6 Hz, 2H) (*C*H). $^{13}C\{^1H\}$ NMR (50.3 MHz, 20 °C, C_6D_6): δ 71.20, 70.09, 69.99, 69.45 (*C*H, integration = 4:1:2:2); 26.79, 26.73, 26.35, 25.99 (CH_3). ^{13}C CP MAS NMR: δ 72.51, 72.03, 71.25, 70.86, 69.99 (CH_3); 29.40, 29.11, 28.72, 28.53, 28.14, 27.75, 27.46, 26.98, 26.39, 25.42 (CH_3). ^{113}Cd NMR: δ 53.21. ^{113}Cd CP MAS NMR: δ 40.97.

$[\{Cd(OPr^i)_3\}Ba\{Hf_2(OPr^i)_9\}]_2$ (4). A toluene (30 mL) solution of $ICdHf_2(OPr^i)_9$ (1.96 g, 1.74 mmol) was added to a suspension of $KBa(OPr^i)_3$[1] (0.62 g, 1.75 mmol) in toluene with continuous stirring, and the resulting reaction mixture was stirred at room temperature for ~12 h. After the filtration of KI, the clear solution obtained was stripped to dryness *in vacuo* to obtain a white solid (2.2 g, 97%). The product could be recrystallized from a mixture of toluene−pentane at −8 °C to obtain transparent platelets of $[\{Cd(OPr^i)_3\}Ba\{Hf_2(OPr^i)_9\}]_2$ in 40% yield which is reduced due to the high solubility and sensitivity of **4** toward the temperature of crystallization. Anal. Calcd for $C_{72}H_{168}Ba_2Cd_2O_{24}Hf_2$: C, 32.86; H, 6.43. Found: C, 32.90; H, 6.65. Mol. Wt. Calcd for **4**: 2632. Found: 2369. ^{1}H NMR (200.13 MHz, 20 °C, C_6D_6): δ 1.36 (d, $^3J_{H-H}$ = 6 Hz, 24H), 1.39 (d, $^3J_{H-H}$ = 6 Hz, 24H), 1.46 (d, $^3J_{H-H}$ = 6 Hz, 12H), 1.47 (d, $^3J_{H-H}$ = 6 Hz, 24H), 1.49 (d, $^3J_{H-H}$ = 6 Hz, 36H), 1.64 (d, $^3J_{H-H}$ = 6 Hz, 24H) (CH_3); methine peaks are observed as three overlapping septets centered at δ 4.50, 4.58, and 4.65. $^{13}C\{^1H\}$ NMR (50.3 MHz, 20 °C, C_6D_6): δ 70.59, 69.21, 68.38, 67.88, 67.70, 65.86 (CH, integration = 8:2:4:4:4:2:4); 27.49, 27.37, 27.12, 26.97, 26.39, 26.28, 26.16 (CH_3, integration = 1:4:6:6:2:1:4). ^{13}C CP MAS NMR: δ 73.72, 73.04, 70.86, 68.48, 64.74, 63.93 (*C*H); δ 33.40, 31.54, 30.95, 30.60, 30.20, 27.55 (CH_3). ^{113}Cd NMR: δ 237.66.

$[\{Cd(OPr^i)_3\}Ba\{Ti_2(OPr^i)_9\}]_2$ (**3**) could be prepared analogously by the reaction (1:1) of $ICdTi_2(OPr^i)_9$ and $KBa(OPr^i)_3$ in toluene. Anal. Calcd for $C_{72}H_{168}Ba_2Cd_2O_{24}Ti_2$: C, 40.96; H, 7.96. Found: C, 41.12; H, 8.05. Mol. Wt. Calcd for **3:** 2109. Found: 1835. ^{1}H NMR (200.13 MHz, 20 °C, C_7D_8): methine peaks are observed as three overlapping septets in the region δ 4.48−5.02; methyl region exhibits six doublets (δ 1.30, 1.37, 1.42, 1.50, 1.52, 1.75) which integrate approximately 1:2:2:3:2:2. ^{13}C $\{^1H\}$ NMR (50.3 MHz, 20 °C, C_7D_8): δ 78.06, 76.33, 72.91, 72.53, 71.67, 70.97, 66.23 (*C*H); 30.34, 29.66, 28.67, 27.44, 27.14, 26.97, 26.54 (CH_3). ^{13}C NMR (CP MAS): δ 78.24, 77.58, 72.48, 71.94, 70.97, 70.61, 66.81, 66.39, 65.96 (*C*H); 31.08, 30.16, 27.98, 27.66, 27.22, 26.83, 25.32 (*C*H3). ^{113}Cd NMR: δ 241.74. ^{113}Cd CP MAS NMR: δ 243.21.

Conclusion

The present work establishes the existence of heterotermetallic alkoxides as unique entities in the solution and solid state which is interesting for the design of molecular precursors to important ternary oxide ceramics, e.g., Y−Ba−Cu, Pb−Mg−Nb. Further it demonstrates the potential of employing coordinatively unsaturated species like $Ba(OPr^i)_3^-$ in building molecular and stoichiometrically well-defined heterotermetallic derivatives. The greater oxophilicity and tendency of Ba(II) to achieve higher coordination numbers commands a rearrangement for attaining a structural motif in which barium attains a favorable coordination number. The most largely investigated route to heterometallic systems is the Lewis acid−base reactions between constituent alkoxides which have provided the majority of well-characterized heterobimetallic alkoxy derivatives[5] and have recently been used for the dissolution of polymeric simple alkoxides of d^n transition or p-block metals.[28] However, such reactions are often inoperative and require more soluble oxoalkoxides as the true reactive species which sometimes result in the products with a metal stoichiometry being different than

(27) Vogel, A. I. *A Text Book of Quantitative Analysis*; Longmans: London, 1968.

(28) (a) Daniele, S.; Papiernik, R.; Hubert-Pfalzgraf, L. G.; Jagner, S.; Häkansson, M. *Inorg. Chem.* **1995**, *34*, 628. (b) Teff, D. J.; Huffman, J. C.; Caulton, K. G. *Inorg. Chem.* **1995,** *34*, 2491.

those anticipated in the beginning of the experiment. Moreover, in certain cases these reactions are found to be selective where the attempted synthesis of a heterotermetallic alkoxide employing three different constituent alkoxides result in an unreacted homometallic and a heterobimetallic alkoxide or a mixture of two heterobimetallic alkoxides.[29] In view of the above, metathesis reactions between well-characterized halobimetallic precursors and novel alkali metal alkoxometalates appear to be stoichiometrically precise for a directed synthesis of heterotermetallic alkoxides. The elimination of salt acts as a driving force, providing controlled synthesis of a heteropolymetallic alkoxide system, which is a primary requirement if single source precursors are to become an advantage for stoichiometric control of resultant oxide materials.

Acknowledgment. We thank the DFG and Fonds der Chemischen Industrie for financial support and Dr. Michael Zimmer for recording the solid state NMR spectra. S.M. gratefully acknowledges the Alexander von Humboldt-Stiftung, Bonn, for the award of a research fellowship.

Supporting Information Available: X-ray crystallographic files in CIF format for compounds **1**−**4** are available on the Internet only. Access information is given on any current masthead page.

IC960116P

(29) Veith, M.; Hans, J.; Stahl, L.; May, P.; Huch, V.; Sebald, A. *Z. Naturforsch.* **1991,** *46b*, 403 and references cited therein.